JOURNAL OF CATALYSIS 111, 243–253 (1988)

Vapor-Phase Catalytic Hydrodeoxygenation of Benzofuran

MINDY C. EDELMAN, MICHAEL K. MAHOLLAND, ROBERT M. BALDWIN, AND SCOTT W. COWLEY*

*Department of Chemical Engineering and Petroleum Refining and *Department of Chemistry, Colorado School of Mines, Golden, Colorado 80401*

Received December 1, 1986; revised November 17, 1987

The catalytic hydrodeoxygenation (HDO) of benzofuran was examined at 300 to 400°C and 35 atm total pressure over a presulfided $NiMo/\gamma\text{-}Al_2O_3$ catalyst. Results from a continuous, plug-flow microreactor operated in the integral (high-conversion) mode show that the benzofuran reaction network includes initial hydrogenation and hydrogenolysis to the oxygenated intermediates 2,3-dihydrobenzofuran, *o*-ethyl phenol, and phenol. The major products formed from subsequent HDO of the phenols are ethylbenzene, toluene, benzene, and ethylcyclohexane. Kinetic analysis shows that hydrogenation of benzofuran may be modeled as pseudo-first order in benzofuran concentration. The HDO reaction shows non-first-order kinetics, and may be modeled as −1 order in oxygenated compounds. The activation energies for the steps of hydrogenation and HDO are lower than those previously reported in the literature for benzofuran HDO over a presulfided $CoMo/\gamma\text{-}Al_2O_3$ catalyst.

INTRODUCTION

Products derived from coal, oil shale, tar sands, and biomass contain various oxygenated, nitrogenated, and sulfated organic compounds. During the catalytic hydroprocessing of these liquid feedstocks, the heteroatoms are removed by the simultaneous reactions of hydrodeoxygenation (HDO), hydrodesulfurization (HDS), and hydrodenitrogenation (HDN). Extensive research has been performed to date in the areas of HDS and HDN, primarily due to environmental concerns to limit SO_2 and NO_x emissions and to industrial concerns to remove potential poisons for downstream refinery catalysts. However, HDO has not received as much attention because of the small amounts of oxygen found in conventional crudes.

With increasing production of synthetic fuels, oxygen removal is receiving greater attention. The major problems associated with the presence of oxygen are the instability of the liquid during storage, poor combustion properties, and the formation of deposits upon combustion. In addition, during conventional refinery hydrotreating processes, the removal of oxygen occurs simultaneously with HDS and HDN. The oxygen-containing compounds compete with the other heteroatom-containing molecules for catalytic sites, and consume additional hydrogen during processing.

Several studies reported in the recent literature describe the HDO of model oxygenated compounds, either alone or in mixtures with sulfated and/or nitrogenated species. The mechanism of HDO has been reported for dibenzofuran (*1, 2*), 1-naphthol (*3*), cresols (*4*), furan (*5*), and recently for benzofuran (BF) by Lee and Ollis (*6*). Most studies show that oxygen removal may occur by the dual paths of direct HDO as well as by initial aromatic ring saturation followed by HDO. The prevalence of the HDO path observed depends upon the compound type and the reaction conditions.

Studies of mixtures of model compounds include those by Rollman (*7*), Furimsky (*5*), Satterfield and Yang (*8*), Lee and Ollis (*9*), and Odebunmi and Ollis (*10, 11*). In general, the presence of N-containing com-

0021-9517/88 $3.00

pounds decreases the rate of HDO due to the poisoning effects of the basic N species. The presence of sulfated compounds may have either a beneficial or an inhibiting effect upon the rate of HDO, depending upon the relative concentrations of S and O.

Lee and Ollis (*6*) used the CoMo/γ-alumina catalyst American Cyanamid HDS-2A in a trickle-bed reactor. The authors obtained differential benzofuran conversions at temperatures from 220 to 345°C and at a H_2 pressure of 69 atm. The observed reaction products included 2,3-dihydrobenzofuran (2,3-DHBF), *o*-ethyl phenol (OEP), ethylbenzene, ethylcyclohexene, and ethylcyclohexane. Phenol, benzene, and toluene were not reported. The authors determined that HDO of BF proceeded by initial hydrogenation to 2,3-DHBF, followed by formation of OEP and subsequent deoxygenation.

The kinetic models derived by Lee and Ollis (*6*) for benzofuran hydrogenation and hydrodeoxygenation were first order in the reacting species. The authors determined an activation energy of 19.4 kcal/mol for hydrogenation and 33 kcal/mol for HDO. A separate set of tests with OEP as feed revealed an activation energy of 16.8 kcal/mol for the HDO of OEP.

EXPERIMENTAL METHODS

Equipment

The HDO studies were carried out in a continuous-flow, fixed-bed catalytic reactor system. Purified hydrogen carrier gas, regulated by a Brooks 5871A Mass Flow Controller, flowed through heat-traced lines to a heated mixing tee. At the tee, liquid feed was introduced and vaporized. The liquid feed, consisting of 10 wt% benzofuran, 3 wt% dimethyl sulfide (sulfiding agent), and 87 wt% *n*-heptane as solvent, was pumped by a Milton Roy minipump.

The reactor, made of $\frac{1}{2}$-in. stainless-steel tubing, was heated by a Lindberg 54032 furnace, controlled by a Leeds and Northrup Electromax V temperature controller. Gas-phase products from the reactor bottom flowed through a regulating valve to the condensing system, which was a Pyrex vacuum trap cooled by a bath of ethylene glycol, ice, and dry ice to an average temperature of −20°C. Uncondensed product flow was measured with a soap bubble meter.

Liquid products were analyzed with a HP 5750 gas chromatograph, using a 10-ft, packed glass column of 10% SP-1000 on 80/100 Supelcoport. The temperature program ran from 30°C (after 2 min isothermal) to 215°C, at 20°C/min. The oven was held at 215°C until analysis was complete. Identification of liquid constituents was also performed with a HP5890 GC/5970 Mass Selective Detector (GC/MS).

Chemical Analyses and Catalyst Characterization

A single charge of 0.15 g of the NiMo/γ-alumina catalyst, crushed and sieved to −25/+35 mesh, was used for all tests. The catalyst, American Cyanamid HDN-30, was sent to the Phillips Petroleum Research and Development Center for chemical and physical analyses prior to usage. The catalyst characteristics are summarized in Table 1. The catalyst was presufided prior to use by heating in a 200 psig, 10% H_2S/H_2 stream at 205°C for 2 h, and then at 405°C for 2 hours.

TABLE 1

HDN-30 Catalyst Analysis

Chemical composition (wt%)	Ni	3.4
	Mo	11.73
	P	3.60
	Al	31.12
Surface area (m^2/g)		179
Pore volume (ml/g)		0.91
Average pore diameter (Å)		203
Average bulk density (g/cm^3)		0.832
Skeletal density (g/cm^3)		3.4125

Both the *n*-heptane and the dimethyl sulfide were from Aldrich, at 99+% purities. The benzofuran was either from Aldrich or from Lancaster Synthesis, LTD., at respective purities of 99.5+% and 99+%. The benzofuran from both suppliers formed a white precipitate upon addition to the solvent, *n*-heptane. The nature of this precipitate was not determinable by GC/MS; however, a substance other than benzofuran and heptane was observed by LC analysis. When the benzofuran was purified by distillation, the distillate was completely soluble in *n*-heptane at 10 wt% benzofuran. The purity of the resulting benzofuran/*n*-heptane mixture used for this study was verified by GC/MS.

Pretesting

A series of preliminary runs were performed to ensure that the reactor system without catalyst was inert to heptane and benzofuran thermal cracking and/or thermal HDO. Results showed that heptane cracking was less than 1.1 wt% under the most severe conditions, and decreased to less than 1 wt% for a mixture of heptane and benzofuran.

From preliminary rate data, calculations were made by Edelman (*12*) to determine whether heat and/or mass transfer limitations could be significant within the reactor. These calculations showed that both external and intraparticle temperature and reactant concentration gradients were negligible.

Procedure

An experimental run consisted of determination of steady-state product distributions for the benzofuran feed at one of four different feed rates, for constant reactor temperature, pressure, and feed composition. The run temperatures studied were 300, 350, and 400°C, and the space times (W/F) were 20, 60, 100, and 140 h-g cat/mol BF. The feed composition was 10 wt% BF, and total system pressure was maintained constant at 34.8 atm (500 psig). The hydrogen-to-feed ratio was kept constant at the equivalent of 5000 SCF/bbl feed. A standard set of run conditions, chosen at 350°C and W/F of 140 h-g cat/mol BF, was periodically repeated to check for catalyst deactivation.

Each run was started by heating the reactor to temperature under a 10% H_2S/H_2 purge, and then initiating liquid feed flow. Next, gas flow was switched to H_2 and the system pressurized to 34.8 atm. After hydrogen and liquid feed rates were established and maintained for a minimum of 1 h, liquid samples were collected, weighed, and analyzed for $\frac{1}{2}$-h periods. Steady-state conditions were determined to exist when a minimum of three consecutive liquid samples showed major component peaks on the GC with a random standard deviation of less than 3% of the peak area.

After a set of steady-state liquid samples was obtained, the feed rates were changed, and after a 1-h reequilibration period, another set of samples were taken. This procedure was repeated for each of the feed rates studied, usually in the sequence of lowest to highest feed rate. The standard run conditions were typically repeated at the beginning or the end of a day's set of runs. If catalyst deactivation was observed from the standard runs, the catalyst was resulfided using the procedure for presulfiding.

The averages of three GC analyses for each liquid sample were then averaged for each steady-state run and converted from wt% to the equivalent mol% distribution. The product distribution was then calculated for each set of reaction conditions.

RESULTS

The HDO of benzofuran was studied at 300, 350, and 400°C, and at space times of 20, 60, 100, and 140 h-g cat/mol BF. The matrix of 12 runs performed at these conditions was used for kinetic modeling.

Liquid product compositions were normalized to a solvent-free basis. Distribution of the oxygenated compounds is listed in

TABLE 2

Oxygenated Distribution during HDO of Benzofuran

W/F (h-g cat/mol BF)	Temperature (°C)	Concentration (mol%)			
		BF	2,3-DHBF	OEP	Phenol
20	300	95.96	2.08	1.44	0.19
60	300	86.41	6.16	5.30	0.40
100	300	78.93	9.16	9.54	0.65
140	300	71.65	10.81	14.29	1.05
20	350	84.86	3.01	8.02	1.23
60	350	67.05	3.32	21.34	3.29
100	350	52.18	2.93	29.35	6.99
140	350	38.79	2.19	33.07	9.45
20	400	79.27	2.37	10.61	3.64
60	400	52.96	2.02	17.71	9.83
100	400	35.30	1.64	17.59	11.05
140	400	22.54	0.90	11.15	5.19

Table 2. Full data are given elsewhere (*12*). The formation of 2,3-dihydrobenzofuran prior to that of *o*-ethyl phenol is indicated from the low-temperature (300°C), low-space-time data in Table 2. At 400°C, the concentrations of the oxygenated intermediates were observed to peak (as they formed) and then decline (as they reacted) with increasing space time.

The major deoxygenated products observed were ethylbenzene and ethylcyclohexane, with lesser amounts of toluene and benzene. At 400°C, the deoxygenated product diethylbenzene, present in the *ortho, meta* and *para* isomers, was observed.

Catalyst Deactivation

The catalyst change in activity with time is shown in Fig. 1. The initial 40 h of catalyst time on-stream was used in pretest runs; the data shown after 40 h represent those runs performed under the standard conditions. From Fig. 1, a gradual decrease in activity is observed, especially for runs after 110 h on-stream. Although the catalyst was resulfided periodically, the original activity could not be restored. The 12-run matrix used for kinetic modeling was performed in the on-stream time period of 40 to 134 h.

DISCUSSION

Based on the observed reaction products, a proposed reaction network for the hydrogenation and subsequent hydrodeoxygenation of BF over a Ni–Mo/γ-Al_2O_3 catalyst is shown in Fig. 2. This mechanism differs from that proposed by Lee and Ollis (*6*) with the inclusion of *o*-ethyl phenol cracking to form phenol, which subsequently undergoes HDO to benzene. Also, the cracking of ethylbenzene to toluene was not observed by Lee and Ollis (*6*).

Although the individual reaction steps

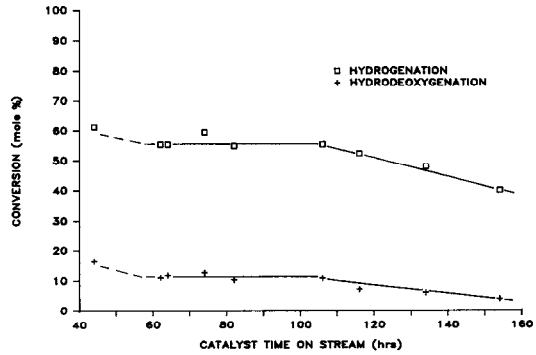

FIG. 1. Catalyst activity history: standard conditions of 350°C, W/F = 140 h-g cat/mol BF.

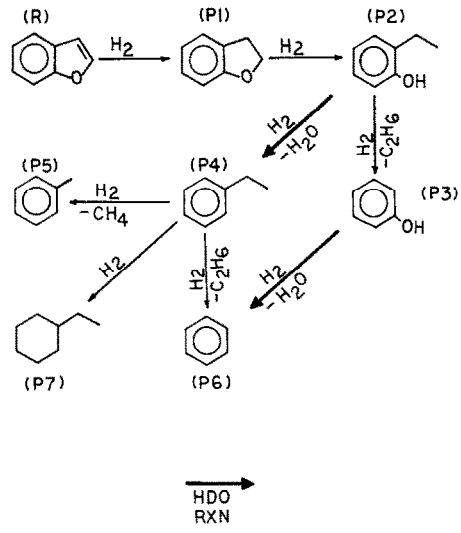

FIG. 2. Proposed reaction network for the hydrodeoxygenation of benzofuran.

were not examined in the present study, it appears reasonable to assume that in the temperature range 300 to 400°C, the hydrogenolysis of 2,3-DHBF is irreversible. This was observed for the catalyst HDS-2A (*6*).

The reaction network of Fig. 2 may be described by two separate models. The hydrogenation route describes the disappearance of BF by hydrogenation to 2,3-DHBF. The HDO route (shown by heavy-set arrows in Fig. 2) describes the combined HDO of all oxygenated organic compounds to form deoxygenated products. These two models are developed in the following sections, incorporating the compound nomenclature of Fig. 2.

Hydrogenation of Benzofuran

Based on adsorption measurements by Sonnemans *et al.* (*13*), it has been postulated by several researchers (*6*, *14*) that on alumina-supported metal oxide catalysts, hydrogen and heteroatom-containing compounds adsorb on different catalyst sites. For the benzofuran system, on one site we postulate competitive adsorption of reactant (R), oxygenated intermediates (P_1, P_2, P_3), water (w), and trace mercaptan (s). Using a Langmuir–Hinshelwood kinetic adsorption model and assuming that the surface reaction of hydrogenation is first order in R and is the rate-controlling step, we obtain

$$r_{hyd} = \frac{k''_{hyd} P_R}{1 + K_R P_R + K_s P_s + K_w P_w + \Sigma_i K_{P_i} P_{P_i}} \quad (1)$$

where k''_{hyd} is a function of temperature, catalyst type, and hydrogen partial pressure and

P_R = partial pressure of R in gas phase at catalyst surface
P_w = partial pressure of water
P_s = partial pressure of sulfur compounds
P_{P_i} = partial pressure of oxygenated organic intermediates P_1, P_2, P_3
r_{hyd} = rate of disappearance of R due to hydrogenation

For an ideal plug-flow reactor, the mass conservation equation for R is

$$r_{hyd} = \frac{-F}{P_{R,0}} \cdot \frac{dP_R}{dW} \quad (2)$$

where

F = inlet molar flow rate of R
W = weight of catalyst in packed bed
$P_{R,0}$ = inlet partial pressure of R

Combination of Eqs. (1) and (2) with rearrangement yields

$$\frac{-d(P_R/P_{R,0})}{d(W/F)} = \frac{k''_{hyd} P_R}{1 + K_R P_R + K_s P_s + K_w P_w + \Sigma_i K_{P_i} P_{P_i}} \quad (3)$$

Equation (3) represents the full psuedo-first-order model for benzofuran hydrogenation. It is general practice in the literature to obtain more tractable forms with the use of several assumptions. Based on findings by Singhal *et al.* (*14*) that dibenzothiophene and H_2S binding strengths are nearly identi-

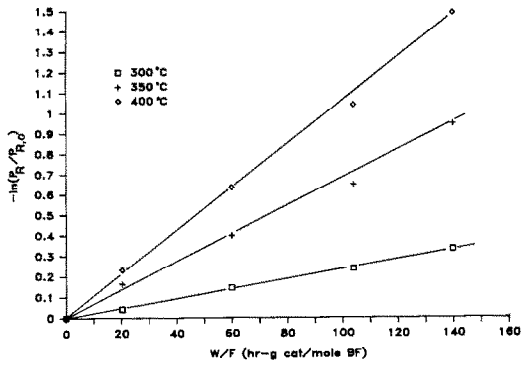

FIG. 3. Test of first-order benzofuran hydrogenation model.

cal, Lee and Ollis (*6*) proposed that water and organic oxygenates bind with similar strengths, so that $K_{P_i} \cong K_w \cong K_R$. Similarly, Miller and Hineman (*15*) modeled quinoline HDN by assuming that the adsorption constants for all organic nitrogen species were equal, although they assumed that the product ammonia bound more weakly to the catalyst ($K_N \gg K_{ammonia}$). This assumption was based on studies of organic amines and ammonia bonding to CoMo catalysts (*13*). Without additional information, the similar assumptions of equal adsorption equilibrium constants for oxygenated organic species and a lower adsorption constant for water are retained in this work.

From an overall oxygen balance, we note that $P_{R,0} = P_R + P_w + \Sigma_i P_{P_i}$, where P_i are the oxygenated organic compounds for $i = 1, 2, 3$. When benzofuran hydrogenation predominates, the concentration of water will be negligible and we may approximate $P_{R,0} \cong P_R + \Sigma_i P_{P_i}$. Using the assumption that $K_{P_i} \cong K_R \gg K_w$, Eq. (3) becomes

$$\frac{-d(P_R/P_{R,0})}{d(W/F)} = \frac{k''_{hyd} P_R}{1 + K_s P_s + K_R P_{R,0}}. \quad (4)$$

In the present study, the inlet concentration of dimethyl sulfide was kept constant and is presumed to remain constant throughout the bed, since the catalyst was presulfided. Because the reactions are mildly exothermic, and the mass of the catalyst bed is small compared with that of the furnace, the reactor bed is assumed isothermal. Therefore, the denominator of Eq. (4) is composed of constant terms; thus

$$\frac{-d(P_R/P_{R,0})}{d(W/F)} = k_{hyd}(P_R/P_{R,0}) \quad (5)$$

where

$$k_{hyd} = \frac{k''_{hyd} P_{R,0}}{1 + K_s P_s + K_R P_{R,0}}.$$

Equation (5) is analytically integrated to provide

$$-\ln(P_R/P_{R,0}) = k_{hyd}(W/F) \quad (6)$$

$$P_R/P_{R,0} = \exp(-k_{hyd}(W/F)). \quad (7)$$

The essentially linear relationship of $\ln(P_R/P_{R,0})$ and W/F is shown in Fig. 3 for the data from the 12-run matrix. The hydrogenation rate constants obtained are listed in Table 3. Analysis of rate constant–temperature dependency, shown in Fig. 4, yields a hydrogenation activation energy of 11.76 kcal/mol. Predicted values of $P_R/P_{R,0}$ are shown along with the experimental data in Fig. 5. The model predictions appear quite satisfactory.

Hydrodeoxygenation

By defining HDO as the rate of formation of deoxygenated organic products (excluding products such as ethane which are formed by cracking) or equivalently as the rate of disappearance of oxygenated compounds,

TABLE 3

Benzofuran Hydrogenation Rate Constants: Psuedo-First-Order Model, Eq. (5)

Temperature (°C)	$k_{hyd} \times 10^3$[a] (mol BF/h-g cat)	r^2
300	2.3524 ± 0.1194	0.999
350	6.6423 ± 0.3481	0.999
400	10.7704 ± 0.5218	0.999

[a] Error bounds are 95% confidence limits on the values of k_{hyd}.

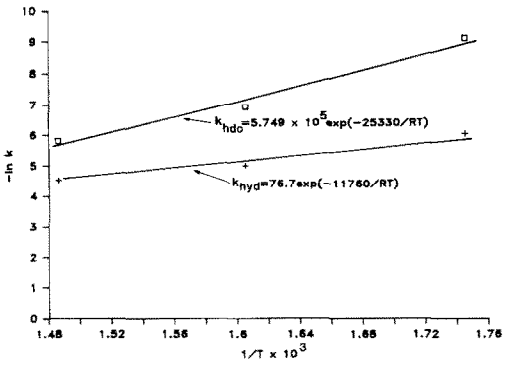

FIG. 4. Arrhenius plots for BF hydrogenation (k_{hyd}) and HDO (k_{hdo}).

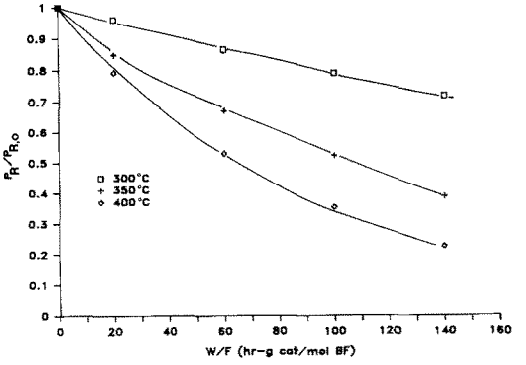

FIG. 5. Comparison of experimental and predicted benzofuran hydrogenation.

$$r_{hdo} = \frac{dP_{deox}}{d(W/F)} = \frac{-dP_{ox}}{d(W/F)}$$

where

$$P_{deox} = P_4 + P_5 + P_6 + P_7$$

$$P_{ox} = P_R + P_1 + P_2 + P_3.$$

If the rate of HDO is proposed to be a first-order reaction in oxygenated compounds P_{ox}, and the surface reactions are assumed to be rate controlling, we obtain the analog of Eq. (5):

$$\frac{-d(P_{ox}/P_{R,0})}{d(W/F)} = k_{hdo}(P_{ox}P_{R,0}) \qquad (8)$$

where

$$k_{hdo} = \frac{k''_{hdo}\, P_{R,0}}{1 + K_s P_s + K_R P_R}.$$

A plot of the experimental data in the form of $-\ln(P_{ox}/P_{R,0})$ versus W/F (Fig. 6) shows that the observed HDO does not follow first-order kinetics, especially at higher temperatures and space times. Since HDO of benzofuran on a HDS-2A catalyst appeared psuedo-first order at temperatures of 345°C and below (*6*), two duplicate runs were made at 400°C to verify the nonlinearity of the first-order plot. Although the catalyst was significantly deactivated for these runs, as shown in Fig. 6 they confirm that the overall HDO reaction does not exhibit first-order kinetics.

The increase in slope of $-\ln(P_{ox}/P_{R,0})$ with increasing W/F shows that k_{hdo} increases as the concentration of oxygenated compounds P_{ox} decreases. This suggests a self-inhibiting effect of the oxygenated compounds. Analysis was made of the simplified rate expression

$$\frac{-d(P_{ox}/P_{R,0})}{d(W/F)} = \frac{k(P_{ox}/P_{R,0})}{1 + K(P_{ox}/P_{R,0})}. \qquad (9)$$

This model results from the full model of Eq. (1), with the assumptions that $K_{P_i} \cong K_R \equiv K$, and that $K \gg K_w$. The assumption that the adsorption constant of water K_w is less than that of the oxygenated organics parallels that used by Miller and Hineman (*15*) for quinoline HDN, as previously discussed. Equation (9) will allow the apparent rate dependency on P_{ox} to vary from 1 if

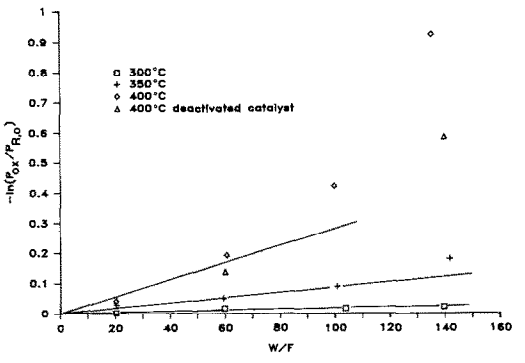

FIG. 6. Test of first-order model for hydrodeoxygenation.

TABLE 4

Nonlinear Regression Fit to Model of Eq. (11)

Temperature (°C)	k	K
300	0.72	71.26
350	4.84	62.97
400	10.29	53.75

$K(P_{ox}/P_{R,0}) \ll 1$ to zero if $K(P_{ox}/P_{R,0}) \gg 1$. When the data were checked for fit to the zero-order model it was evident that the HDO reaction did not follow zero-order kinetics at high temperatures and high space times.

After rejection of the pseudo-first-order and zero-order models for the HDO reaction, the following model was examined:

$$\frac{-d(P_{ox}/P_{R,0})}{d(W/F)} = \frac{k(P_{ox}/P_{R,0})}{(1 + K(P_{ox}/P_{R,0}))^2}. \quad (10)$$

This model may be derived by assuming that the surface reaction rate is proportional to the concentration of adsorbed oxygenated compounds, the adsorbed hydrogen, and also proportional to the number of vacant sites.

The model of Eq. (10) allows the apparent rate dependency on P_{ox} to vary from 1 when $K(P_{ox}/P_{R,0}) \ll 1$ to -1 when $K(P_{ox}/P_{R,0}) \gg 1$. The parameters k and K of Eq. (10) were fit using an IMSL nonlinear regression subroutine to produce the values shown in Table 4. It is evident that $K(P_{ox}/P_{R,0})$ will be much greater than 1, even for the lowest observed value of $P_{ox}/P_{R,0} = 0.4$ at 400°C. The model of Eq. (10) may be simplified by neglecting the 1 in the denominator:

$$\frac{-d(P_{ox}/P_{R,0})}{d(W/F)} = \frac{k/K^2}{P_{ox}/P_{R,0}} = \frac{k_{hdo}}{P_{ox}/P_{R,0}}. \quad (11)$$

Equation (11) is analytically integrated to yield

$$(P_{ox}/P_{R,0})^2 = 1 - 2k_{hdo}(W/F). \quad (12)$$

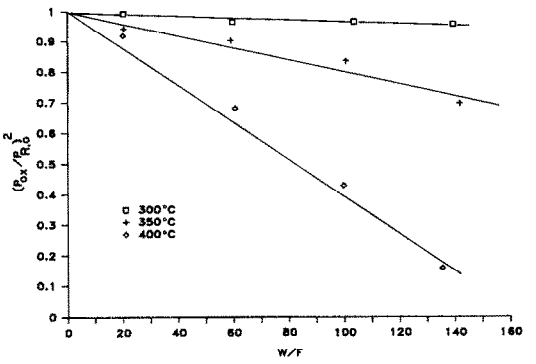

FIG. 7. Test of (−1)-order model for hydrodeoxygenation.

A plot of $(P_{ox}/P_{R,0})^2$ versus W/F appears linear (Fig. 7). Linear regression yielded the values for k_{hdo} and r^2 given in Table 5. The hydrodeoxygenation rate constant–temperature dependency, shown in Fig. 4, yields a hydrodeoxygenation activation energy of 25.33 kcal/mol.

Predicted values of $P_{ox}/P_{R,0}$ are compared with experimental values in Fig. 8. The fit of the (−1)-order model appears satisfactory.

The rates of hydrogenation and hydrodeoxygenation of benzofuran predicted by Eqs. (8) and (11) are compared with those predicted from the data of Lee and Ollis (*6*) for the CoMo catalyst HDS-2A in Figs. 9 and 10. It must be cautioned that their hydrogenation studies with BF were performed at temperatures at and below 260°C and at 69 atm H_2 pressure, while HDO studies were at temperatures from 310 to

TABLE 5

Hydrodeoxygenation Rate Constants: (−1)-Order Model of Eq. (11)

Temperature (°C)	$k_{hdo} \times 10^{3a}$ (mol BF/h-g cat)	r^2
300	0.1114 ± 0.2149	0.4046
350	0.9723 ± 0.2102	0.9819
400	2.9617 ± 0.3153	0.996

[a] Error bounds represent 95% confidence intervals.

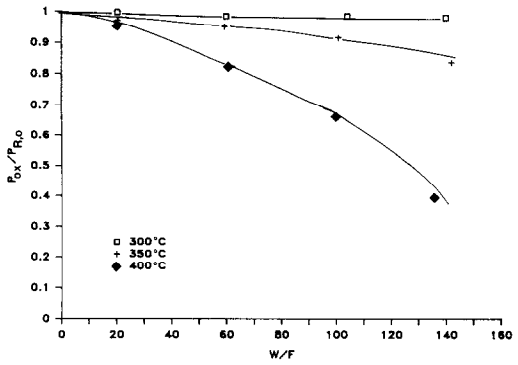

FIG. 8. Comparison of experimental and predicted hydrodeoxygenation.

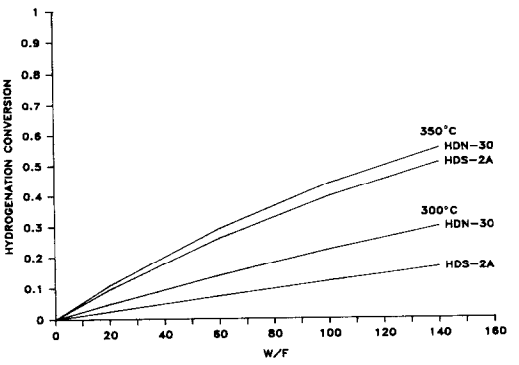

FIG. 9. Comparison of predicted hydrogenation conversions for HDN-30 (present study) and HDS-2A [Lee and Ollis (*6*)].

345°C and at 69 atm. Conversely, in the present study hydrogenation and HDO rates were determined from data at 300 to 400°C and 29 atm of H_2. The higher hydrogen partial pressure used by Lee and Ollis (*6*) is expected to enhance the rates of hydrogenation and HDO.

From Fig. 9 it is evident that the catalyst HDN-30 used in the present study is more active for hydrogenation at 300 and 350°C, when compared with the extrapolated activity for the HDS-2A catalyst. The HDN-30 also appears more active for HDO at 300°C (Fig. 10) and about equally active for HDO at 350°C.

One point of note is that Lee and Ollis (*6*) obtained differential conversions of liquid-phase reactants at temperatures below 345°C, while this study produced integral conversions of gas-phase reactants at temperatures up to 400°C. The marked departure from first-order HDO kinetics was apparent in this study only at the higher temperatures and higher space times. Therefore, a comparison of the relative activities of the two catalysts, which are based on data obtained from different operating ranges, must be regarded as preliminary.

Thermodynamic Equilibrium

The equilibrium constants K_{eq} have been calculated for the reactions shown in Fig. 2. Data for the individual compounds was taken from Stull *et al.* (*16*) when available, from Stein and Barton (*17*), and from Reid *et al.* (*18*). In some instances, thermodynamic properties for the less common compounds were calculated using the method of Benson (*19*).

Figure 11 is a plot of the equilibrium constants versus temperature for the reactions listed in Table 6. Several points are of note:

1. Although styrene formation is thermodynamically favorable at all temperatures used in this study, styrene (the product of direct HDO of benzofuran) was not observed in the reaction products.

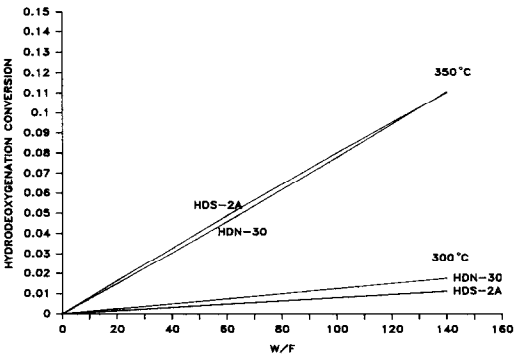

FIG. 10. Comparison of predicted hydrodeoxygenation conversions for HDN-30 (present study) and HDS-2A [Lee and Ollis (*6*)].

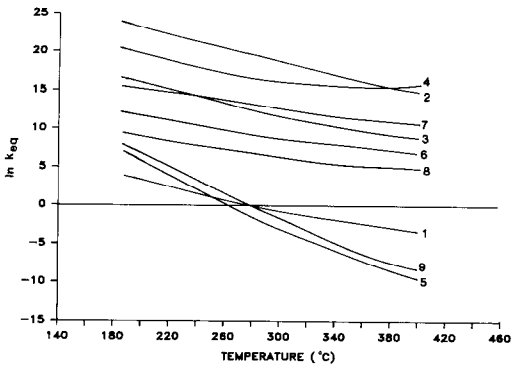

FIG. 11. Equilibrium constants for reactions listed in Table 6.

2. The initial hydrogenation of BF to 2,3-DHBF is thermodynamically unfavorable; therefore, the role of the catalyst is to enhance the kinetics of this first step in the reaction network.

CONCLUSIONS

The alumina-supported NiMo catalyst HDN-30 shows considerable activity for the hydrogenation and HDO of benzofuran. The benzofuran HDO reaction network includes formation of the oxygenated intermediates 2,3-dihydrobenzofuran, *o*-ethyl phenol, and phenol, with subsequent HDO of these compounds to form ethylbenzene, toluene, and benzene.

Hydrogenation of benzofuran may be satisfactorily modeled as psuedo-first order in benzofuran concentration. HDO may be modeled as −1 order in concentration of oxygenated organic compounds. These models are developed from Langmuir–Hinshelwood mechanisms that assume that the adsorption equilibrium constants of oxygenated organic species are comparable and higher than that of water.

The HDN-30 catalyst appears more active at temperatures of 300 to 350°C than the CoMo catalyst HDS-2A. The HDN-30 catalyst showed a hydrogenation activation energy of 11.76 kcal/mol and a HDO activation energy of 25.33 kcal/mol, compared with 19.40 and 33.00 kcal/mol, respectively, for the catalyst HDS-2A (*6*).

The catalyst HDN-30 shows significant cracking activity, with the production of phenol and toluene observed at temperatures as low as 300°C. In addition, the catalyst exhibits alkylation activity at 400°C, as seen by the formation of diethylbenzene.

TABLE 6

Reactions Corresponding to Fig. 11

(1) BF + H_2 = 2,3-DHBF
(2) BF + $2H_2$ = styrene + H_2O
(3) 2,3-DHBF + H_2 = OEP
(4) OEP + H_2 = ethylbenzene + H_2O
(5) OEP + $3H_2$ = ethyl cyclohexanol
(6) OEP + H_2 = phenol + C_2H_6
(7) Ethylbenzene + H_2 = toluene + CH_4
(8) Ethylbenzene + H_2 = benzene + C_2H_6
(9) Ethylbenzene + $3H_2$ = ethylcyclohexane

REFERENCES

1. Hall, C. C., and Cawley, C. M., *J. Soc. Chem. Ind.* **58,** 7 (1939).
2. Krishnamurthy, S., Panvelker, S., and Shah, Y. T., *AIChE J.* **27,** 994 (1981).
3. Li, C.-L., Cao, Z.-A., and Gates, B. C., *AIChE J.* **31,** 170 (1985).
4. Odebunmi, E. O., and Ollis, D. F., *J. Catal.* **80,** 56 (1983).
5. Furimsky, E., *Appl. Catal.* **6,** 159 (1983).
6. Lee, C.-L., and Ollis, D. F., *J. Catal.* **87,** 325 (1984).
7. Rollmann, L. D., *J. Catal.* **46,** 243 (1977).
8. Satterfield, C. N., and Yang, S. H., *J. Catal.* **81,** 335 (1983).
9. Lee, C.-L., and Ollis, D. F., *J. Catal.* **87,** 332 (1984).
10. Odebunmi, E. O., and Ollis, D. F., *J. Catal.* **80,** 65 (1983).
11. Odebunmi, E. O., and Ollis, D. F., *J. Catal.* **80,** 76 (1983).
12. Edelman, M. C., "Vapor Phase Catalytic Hydrodeoxygenation of Benzofuran in a Flow Microreactor," T-3103, Arthur Lakes Library, Colorado School of Mines, 1985.
13. Sonnemans, J., van den Berg, G. H., and Mars, P., *J. Catal.* **31,** 220 (1973).
14. Singhal, G. H., Espino, R. L., and Sobel, J. E., *J. Catal.* **67,** 446 (1981).
15. Miller, J. T., and Hineman, M. F., *J. Catal.* **85,** 117 (1984).

16. Stull, D. R., Westrum, E. F., and Sinke, G. C., "The Chemical Thermodynamics of Organic Compounds." Wiley, New York, 1969.
17. Stein, S. E., and Barton, B. D., *Thermochim. Acta* **44,** 265 (1981).
18. Reid, R. C., Prausnitz, J. M., and Sherwood, T. K., "The Properties of Gases and Liquids." McGraw–Hill, New York, 1977.
19. Benson, S. W., "Thermochemical Kinetics." Wiley, New York, 1968.